Robust Method for Detecting Defect in Images Printed on 3D Micro-textured Surfaces: Modified Multiple Paired Pixel Consistency

Sheng Xiang[1], Shun'ichi Kaneko[1] and Dong Liang[2]
[1]*Graduate School of Information Science and Technology, Hokkaido University, Sapporo, Japan*
[2]*College of Computer Science and Technology, Nanjing University of Aeronautics and Astronautics, Nanjing, P. R. China*

Keywords: Defect Inspection, Multiple Paired Pixel Consistency, Orientation Code, Qualification of Fitting, Data Filtering, 3D Micro-textured Surface.

Abstract: When attempting to examine three-dimensional micro-textured surfaces or illumination fluctuations, problems such as shadowing can occur with many conventional visual inspection methods. Thus, we propose a modified method comprising orientation codes based on consistency of multiple pixel pairs to inspect defects in logotypes printed on three-dimensional micro-textured surfaces. This algorithm comprises a training stage and a detection stage. The aim of the training stage is to locate and pair supporting pixels that show similar change trends as a target pixel and create a statistical model for each pixel pair. Here, we introduce our modified method that uses the chi-square test and skewness to increase the precision of the statistical model. The detection stage identifies whether the target pixel matches its model and judges whether it is defective or not. The results show the effectiveness of our proposed method for detecting defects in real product images.

1 INTRODUCTION

Defect inspection has always played a key role in the manufacturing quality control (QC) process. Therefore, many studies have focused on automatic quality inspection based on computer vision. In this paper, our interest is in assessing how the currently available visual inspection systems perform various QC checks on printed products. We consider mainly the inspection of printed characters and text or logotypes for defects, such as holes, dents, and foreign objects (Mehle et al., 2016). Currently, QC in the printing industry is often carried out manually, but it is labor-intensive and time-consuming process. Additionally, results can vary according to inspectors' mood, experience, and individual level of skill. Thus, manual QC checks can be unreliable. Furthermore, no operator-independent quality standard has been established. To overcome these problems, manual inspection is beginning to be replaced by automatic visual inspection systems (Ngan et al., 2011).

Texture is one of the most important features for detecting defects and the issues that arise with defect detection are generally considered to be due to problems with texture analysis. Texture analysis techniques may be categorized, as reported by Xie (Xie, 2008): statistical techniques (Karimi and Asemani, 2013), structural techniques (Kasi et al., 2014), filter-based techniques (Jing et al., 2015), and model-based techniques (Li et al., 2015).

In this paper, we analyze the surface of a printed product embossed with randomly distributed three-dimensional (3D) micro-textures. These types of surface are achieved by an embossing process. Embossing is the process of making tiny raised and concave patterns on the surface of metal, plastic or other materials. These embossed surfaces have an attractive appearance, good hand feel and excellent slip resistance. Therefore, these surfaces have been widely used in many products worldwide. These three-dimensional (3D) micro-structures, which are uniformly embossed on the surface, produce a slight shadow under illumination and appear as a random texture in their image. Fluctuations in illumination greatly influence the imaging effect of the surface. To overcome this problem, we use our previously proposed approach of orientation code matching (Ullah and Kaneko, 2004), which is a robust matching or registration method based on orientation codes. We also analyze printed characters on 3D micro-textured surfaces, which causes statistical fluctuation and thus makes matching or defect registration difficult. From past studies, we have found that points at the same locations in printed characters can show statistical simi-

Xiang, S., Kaneko, S. and Liang, D.
Robust Method for Detecting Defect in Images Printed on 3D Micro-textured Surfaces: Modified Multiple Paired Pixel Consistency.
DOI: 10.5220/0008910002600267
In *Proceedings of the 15th International Joint Conference on Computer Vision, Imaging and Computer Graphics Theory and Applications (VISIGRAPP 2020) - Volume 5: VISAPP*, pages 260-267
ISBN: 978-989-758-402-2; ISSN: 2184-4321

larity so long as the difference between them is specifically defined. The method we propose in the present paper is called the Multiple Paired Pixel Consistency (MPPC) Model in Orientation Codes, which is a modified version of the MPPC. Its effectiveness has already been demonstrated through many experiments (Xiang et al., 2018). Based on the MPPC model of defect-free images, we propose an algorithm for defect inspection.

This paper is organized as follows. Section 2 introduces in detail how the MPPC model works. Section 3 introduces the modification for the MPPC. Section 4 reports the experimental results and compares the performance of the modified MPPC with that of other advanced approaches. Section 5 concludes the paper and addresses future works.

2 MPPC DEFECT-FREE MODEL

In this section, we first introduce the original version of Orientation code and propose signed difference between any two codes as preparation for making a more precise statistical model of their difference. Then we introduce how to make the MPPC model for defect-free logo.

2.1 Orientation Codes

Orientation codes were proposed as filtering to extract robust features based on only orientation information involved in gradient vectors from any general types of pictures. One could utilize it in the design of the robust matching scheme, for example in the original reference (Ullah and Kaneko, 2004).

Let $I(i,j)$ be the brightness of pixel (i,j). Then its partial derivatives in horizontal and vertical directions are written as $\nabla I_x = \partial I/\partial x$ and $\nabla I_y = \partial I/\partial y$, respectively. The orientation angle θ can be computed by $\theta = tan^{-1}(\nabla I_y/\nabla I_x)$ of which actual orientation is determined after checking signs of the derivatives, thus making the range of θ to be $[0,2\pi)$. The orientation code or OC is obtained by quantifying the orientation angle θ into N levels with a constant width $\Delta\theta\,(=2\pi/N)$. The OC can be expressed as follows.

$$C_{i,j} = \begin{cases} \left\lfloor \frac{\theta_{i,j}}{\Delta\theta} \right\rfloor & |\nabla I_x| + |\nabla I_y| \geq \Gamma \\ N & \text{otherwise} \end{cases} \quad (1)$$

where Γ is a threshold level for ignoring pixels with low-contrast neighborhoods. That is, pixels with neighborhoods of enough contrast are assigned OC from the set $\{0,1,\ldots,N-1\}$ while we assign the code N to ignored pixels. In this paper $\Gamma = 10$ and $N = 16$. An example of a set of OCs is shown in Fig. 1.

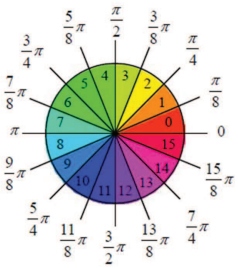

Figure 1: Sixteen-OC.

2.2 Signed Difference in OC

Here we propose a somewhat new definition in OC space which is better suited for the more detailed statistical design than the original one. In contrast with the previous definition (Ullah and Kaneko, 2004), the definition used here has not only positive differences but also negative ones. We expect it to give a more complete and precise distribution of OC differences that facilitates statistical handling. The expression is

$$\Delta(a,b) = \begin{cases} (a-b)-N & b \leq \left(\frac{N}{2}-1\right) \cap (a-b) \geq \frac{N}{2} \\ (a-b)+N & b > \left(\frac{N}{2}-1\right) \cap (a-b) < -\frac{N}{2} \\ a-b & \text{otherwise} \end{cases} \quad (2)$$

where a and b represent the orientation code to be compared or subtracted, for instance from a target and a reference image, respectively, and N shows the invalid-pixel code.

2.3 MPPC Modeling

Fig. 2 shows the schematic structure of the proposed model 'Multiple Paired Pixel Consistency (MPPC)' which can represent one statistical characteristic in orientation code difference between two elemental pixels in the pairs. The main idea of this statistical modeling of pictures is called 'CP3' that has been proposed previously by Liang (Liang et al., 2015) for robust background subtraction. We propose an extension of this scheme by introducing the cohesive relationship of orientation codes in logo-logo pairs which are defined between each target pixel P on a logotype and the set of its supporting pixels also on the same logotype, which should be selected to have higher consistency or correlation with the target pixel. In other words, all of them have similar trends of change as the target pixel has, for which we can make a statistical model by fitting a single Gaussian distribution to the orientation code difference histogram of these pairs of high consistency.

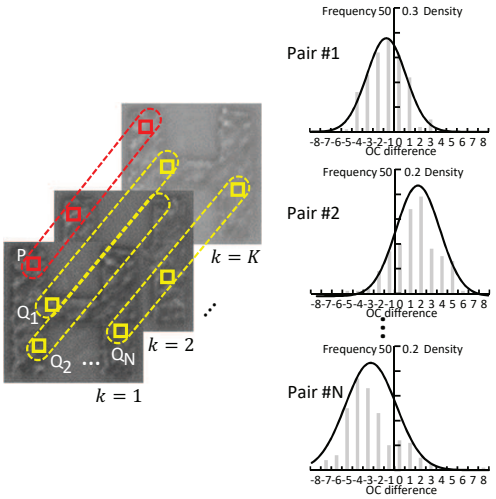

Figure 2: Scheme of MPPC modeling.

We now consider how to select the supporting pixels from all the candidate pixels for a target pixel. For an arbitrary logo-logo pixel pair (P,Q), we have two sets of OC sequences in the same positions in all K training images as follows:

$$\mathbf{P} = \{p_1, p_2, \cdots, p_K\} \tag{3}$$

and

$$\mathbf{Q} = \{q_1, q_2, \cdots, q_K\} \tag{4}$$

where K is a total number of training sample images as shown in Fig. 2.

For formalization in this paper, we use capital letters in boldface, such as $\mathbf{Q}$, to represent any set, simple capital ones to represent any pixel, lower ones to show any orientation codes of the pixels, respectively.

The expectation values and the variances over $\mathbf{P}$ and $\mathbf{Q}$ are defined as $\overline{p} = 1/K\sum_{k=1}^{K} p_k$, $\overline{q} = 1/K\sum_{k=1}^{K} q_k$, $\sigma_{\mathbf{P}}^2 = \frac{1}{K}\sum_{k=1}^{K}(p_k-\overline{p})^2$, and $\sigma_{\mathbf{Q}}^2 = \frac{1}{K}\sum_{k=1}^{K}(q_k-\overline{q})^2$, respectively.

The covariance between $\mathbf{P}$ and $\mathbf{Q}$ is defined as

$$C_{\mathbf{P},\mathbf{Q}} = \frac{1}{K}\sum_{k=1}^{K}(p_k-\overline{p})(q_k-\overline{q}) \tag{5}$$

If $C_{\mathbf{P},\mathbf{Q}} > 0$, then they have a consistency or co-occurrence probability, and in order to measure the consistency quantitatively, we use the Pearson product-moment correlation coefficient:

$$\gamma_{\mathbf{P},\mathbf{Q}} = \frac{C_{\mathbf{P},\mathbf{Q}}}{\sigma_{\mathbf{P}} \cdot \sigma_{\mathbf{Q}}} \tag{6}$$

where $\sigma_{\mathbf{P}}$ and $\sigma_{\mathbf{Q}}$ are the standard deviations of $\mathbf{P}$ and $\mathbf{Q}$, respectively.

For each target pixel $P(u,v)$ at the position (u,v), we may have $M-1$ candidate pixels in the same logotype, where M properly defines the total size of the logotype in pixel. From these candidates we can select $N\,(<M)$ supporting pixels in descending order of the value of $\gamma_{\mathbf{P},\mathbf{Q}}$. The set of N supporting pixels is

$$Q = \left\{ Q_i(u_i,v_i) \,|\, \gamma_{\mathbf{P},\mathbf{Q}_i} \geq \gamma_{\mathbf{P},\mathbf{Q}_{i+1}} \right\}_{i=1,2,\cdots,N} \tag{7}$$

We assume that each supporting pixel Q_i maintains a bivariate OC difference with the target pixel P,

$$\Delta(p,q_i) \sim N(\mu_i,\sigma_i) \tag{8}$$

where $N(\mu_i,\sigma_i)$ is the Gaussian distribution with the mean μ_i and the variance σ_i^2 which are calculated from the corresponding pixel sets $\mathbf{P}$ and $\mathbf{Q}$.

After the modeling for one target pixel P, the above set of N pairs of four parameters for the position u_i, v_i and the two statistical parameters μ_i and σ_i are recorded in a row of a look-up table (LUT). Through the repetition of modeling, the LUT is filled in to include the total set of MPPC models for all of the pixels in an elemental logotype.

2.4 Defect Detection by MPPC

We now discuss how to utilize the proposed MPPC model of the relationship between pixels in the defect-free logotype for detecting many sorts of logotype defects. Since the MPPC model can represent the statistical behavior of the relation of an individual target pixel to the supporting pixels around it, we utilize it to statistically test whether a target pixel is recognized as a reasonable sample from the distribution registered in the LUT or not. The scheme for defect detection algorithm is shown in Fig. 3.

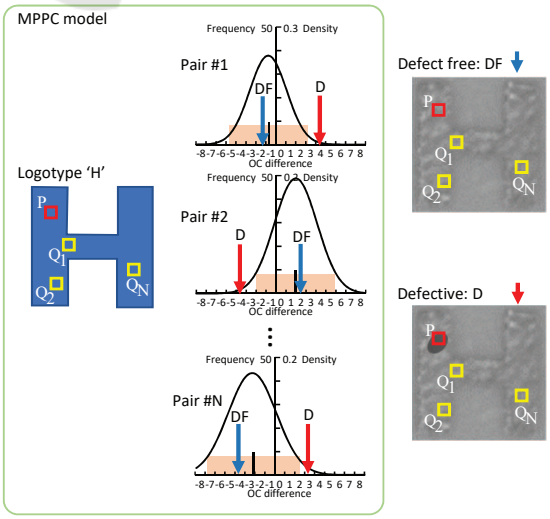

Figure 3: Scheme of defect detection by MPPC model.

Defects have several types, such as dust or particles, scratches, misprinting, hairs, spits, etc., of which characteristics are randomness in alignment, texture, shape, or size. Because of high-performance quality control in production lines, these defects may be very small, and furthermore, we should also keep in mind their very low probability of occurrence. In addition, in this paper we need to handle the randomness in 3D micro-textured surfaces too. Thus, these fundamental characteristics lead us to approaches based on pixel-wise evaluation for detection. Afterwards we may proceed to some next steps to recognize them as aggregated regions that reveal some common characteristics. From these considerations and the investigation in Section 2.3, the two features of our MPPC model, spatial sparseness and high consistency in correlative relation, can be utilized for handling defects. The former may prevent any defect from occupying P and some supporting pixels simultaneously and then by use of the latter feature we expect to have some evaluation scheme for recognizing whether P is occupied by any defect or not.

The next task must be to design a measure for judging defect pixels or defect-free pixels by use of the MPPC model. We first test each OC difference between target pixel P and a supporting pixel Q in the MPPC model or the LUT by using Q for P in the target image. We define the following measure:

$$\beta_i = \begin{cases} 1 & \|\Delta(p,q_i) - \mu_i\| \geq C \cdot \sigma_i \\ 0 & \text{otherwise} \end{cases} \quad (9)$$

for identifying the normal ($\beta_i = 0$) or the abnormal ($\beta_i = 1$) states at the corresponding position defined by the elemental MPPC model, where the constant C is a parameter which can be set from 1 to 3 to define an area for 68% through 99.7% acceptance probability. Finally, we use the total sum

$$\xi = \frac{1}{N}\sum_{i=1}^{N}\beta_i \quad (10)$$

to construct a decision rule for the occupation of P by any defect: $\xi \geq T$, where $T = \frac{1}{N}\left(floor\left(\frac{N}{2}\right)+1\right)$ is a threshold for the general majority rule, and N is the total number of supporting pixels.

3 MODIFICATION OF THE MPPC

Two representative approaches are known for modifying or upgrading the performance of the MPPC model for defect detection. The first modifies the structure and the second modifies the parameters. In this paper, we attempt the first approach by excluding or filtering inappropriate data from the process of making elemental Gaussian models for each pixel pair consisting of a target pixel and a supporting pixel. To realize this process, we need two schemes: a judgment scheme and a localization scheme that locates inappropriate or outlying data.

Fig 4 is an example of simulative detection. We

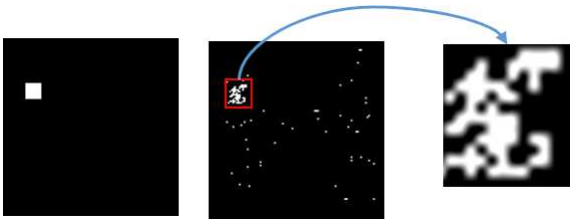

Figure 4: An example of a detection result. From left to right, ground truth image, detection result, magnified view of the defect.

can see that it contains some holes in the defective squared area. We suspect that there may be some problems with the trained model. So we need to analyze the trained model. We randomly select a pixel in the hole and analyze the statistical relationship between the target and its supporting pixels.

Fig 5 is a histogram for one pixel pair that shows

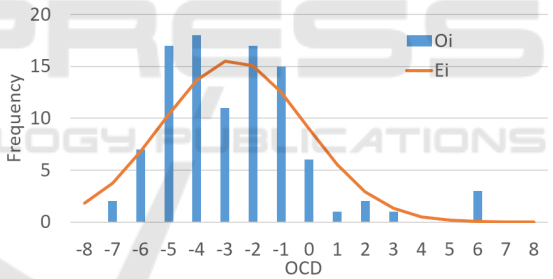

Figure 5: A pixel pair histogram showing frequency of orientation code differences between the target pixel and its supporting pixel.

the frequency of orientation code (OC) differences between the target pixel versus its supporting pixel. Where O_i is the measured data and E_i is the fitted data. From this analysis, we could identify gaps between the fitted distribution and the actual distribution of measured data. The gaps may have been caused by noise (possibly including defects) in the training data, but there were probably quite rare. Detecting defects in the materials examined in this article is not an easy task, even for professional inspectors who are trained to find small and/or obscure defects. Furthermore, judgment may vary depending on the individual inspector. Another problem is that the number of training samples is not so larger in general. If this trial set of samples contains inaccurate data expressed as noise, it may have a not neglectable effect on the

resulting model structure. Therefore, we proposed a process of filtering out these outlying data as a modification of the MPPC model. We hoped that this modification would make a version of the MPPC model that could detect defects more accurately.

The modification process comprises two steps. First, we test the appropriateness of any trained element of the MPPC model; in other words, we determine whether the fit is good. If the fit is poor, we need to proceed with the second step, which comprises filtering inconsistent image data. From the resulting filtered image, we can then create a single elementary Gaussian model to fit the pair of target and supporting pixels again.

3.1 Chi-square Qualification Test

The MPPC model needs many elementary Gaussian distributions for each pixel pair, which are fitted to a set of sample gray levels. In this section, we introduce how to judge fit quality. For every elementary model, we have two histograms. One shows the OC differences for a pixel pair and is called the observation histogram H_O. The other is the expected histogram H_E generated by the MPPC modeling procedure. Here, we introduce Pearson's chi-square test (McHugh, 2013) to measure goodness of fit. The expression is as follows:

$$\chi^2 = \sum_{i=1}^{N} \frac{(O_i - E_i)^2}{E_i} \tag{11}$$

where N is the number of bins in the H_O, O_i is an observed value in the i-th bin of H_O, and E_i is the corresponding expected value in the H_E.

$\chi^2 < p-value$ indicates that the fit is good; otherwise the fit is considered poor, in which case we proceed with the next step of filtering noisy data, and attempt the fit again until we achieve $\chi^2 < p-value$. The $p-value$ can be found in the chi-square table.

3.2 Skewness-based Data Filtering

Fig. 5 shows an example of outlying noisy data in the rightmost bin. The next problem may be how to find the data or position of noisy data. Our MPPC model is based on an approximation via the single Gaussian model, which is symmetrical in nature, so it is difficult to distinguish these biased data in the histogram. To estimate the locations of these data, we introduced a statistical feature, that is, *skewness* (Mardia, 1970), where asymmetry is measured in probability distributions of a real-valued random variable around its mean. Here, we utilize Pearson's moment coefficient of skewness γ_1, defined as:

$$\gamma_1 = E\left[\left(\frac{X-\mu}{\sigma}\right)^3\right] \tag{12}$$

where μ is the mean, σ is the standard deviation, X is the observed value, and E is the expectation operator.

$\gamma_1 < 0$ indicates *negative skew*, which means the left tail in the histogram is longer than the right tail; that is, the mass of the distribution is concentrated on the right of the histogram.

In this case, we may assume that the leftmost columns in histogram H_O include noisy data. Thus, we remove these data or record the identification numbers, including those in the leftmost column in histogram H_O, to create a new histogram $H_O^{'}$. We then perform a single Gaussian fitting based on $H_O^{'}$ to obtain another new MPPC model. Next, we create a new expected histogram $H_E^{'}$ based on the new MPPC model. On the other hand, we must consider *positive skew*, where the right tail is longer than the left tail; that is, the mass of the distribution is concentrated on the left of the histogram. Therefore, we can assume that the rightmost columns in histogram H_O may contain noisy data. We must remove the image data belonging to the rightmost column of histogram H_O, resulting in a new histogram $H_O^{'}$. Finally, we utilize the chi-square qualification test to check the fitting quality of the new MPPC model. This loop operation is continued until the fitting quality improves.

4 EXPERIMENTS

4.1 Experimental Setup

We used six sets of real images from a factory: the characters 'H', 'U', 'A', 'W', 'E', and 'I', each of which includes 160 defect-free images taken under 3 different illumination conditions: dark, normal, and bright. Of these 160 images, we chose 60 to train the MPPC model. In our experiments, we set the two thresholds in the detection stage as $C = 2.0$ and $T = 0.5$.

We used two defect types: synthesized or artificial defects and real defects, as shown in Fig. 6 and Fig. 7, respectively.

Because it was difficult to collect real defects from factories, we instead used synthesized defects in our experiments, as shown in Fig. 7. Here, we first extracted a small square area from the logotype background (unprinted portion) and pasted it onto the logotype (printed portion). These artificial defects represent misprinted logotypes. Fig. 6 demonstrates that

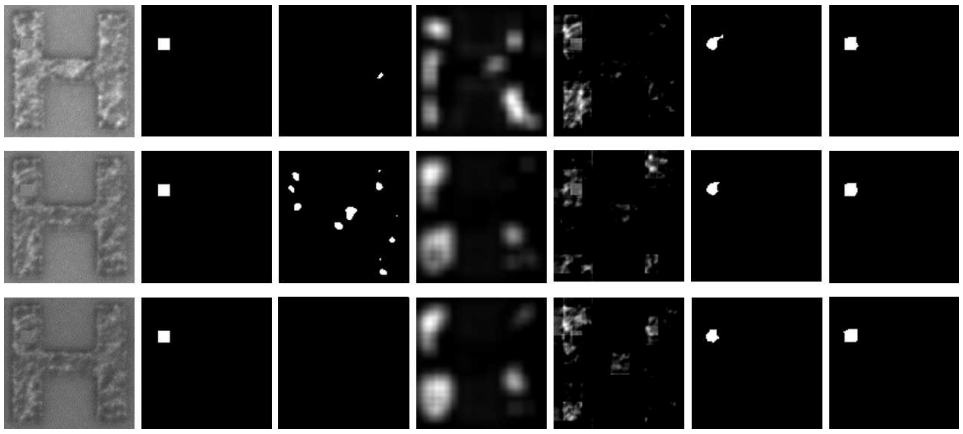

Figure 6: Examples of defect detection results for synthesized defects. From the leftmost to rightmost column: test images, corresponding ground truth images, detected results by phase only transform, prior knowledge guided least squares regression, modified robust principal component analysis with noise term and defect prior, multiple paired pixel consistency (MPPC), and MPPC with modification, respectively.

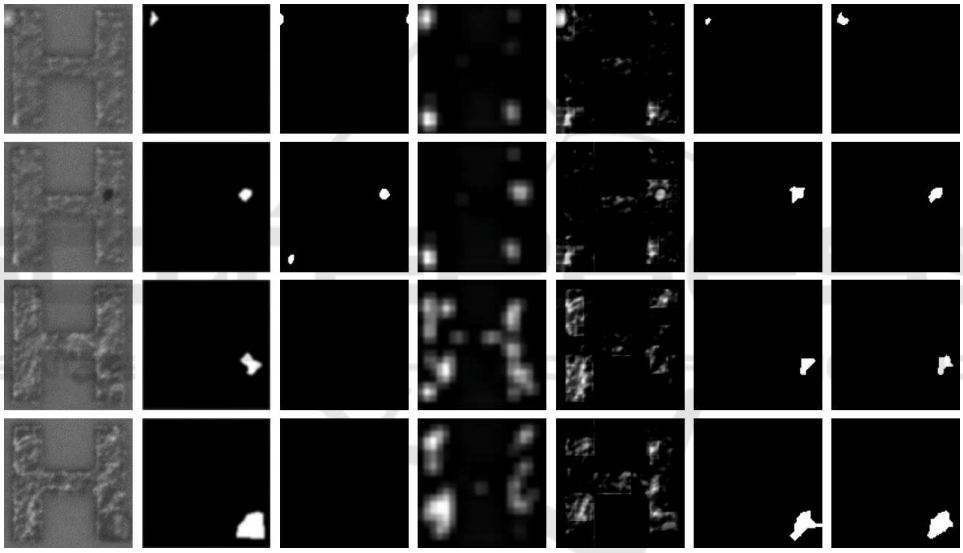

Figure 7: Detected defects in real defect images.

the ground truth can not easily be defined for real defects because the boundary is unclear between the logotype and its background, even with magnification. Therefore, we used the synthesized defects to quantitatively evaluate the performance of the proposed MPPC-based detection method.

4.2 Evaluation Metrics

There are several ways to evaluate the performance of defect detection. First pixel-level precision, recall, and F-measure are tried to test the proposed MPPC models and the detection algorithm for the statistical test based on the models, where our approach assumes as a two-class or binary classification problem to classify any pixel into the defective class and the defect-free class. Along with our problem to detect defects in pixel, we utilized three evaluation metrics: *Precision*(also known as positive predictive value), *Recall* (also known as sensitivity) and *F-measure*. These measures have wide application in pattern recognition, information retrieval, and binary classification. And pixel-level defect detection is a typical binary classification problem, so these three indicators can also be used for the quantitative analysis of defect detection. *Precision* can be considered a measure of accuracy, while *Recall* can be considered a measurement of defect integrity.

F-measure is a harmonic average of the *Precision* and *Recall*.

$$F-measure = \frac{2Precision \cdot Recall}{Precision + Recall} \tag{13}$$

Table 1: Pixel-level based performance of defect detection: comparison of 5 methods.

Defect type	Measurement	PHOT	PG-LSR	PN-RPCA	MPPC	MPPC+Modification
Synthesized	Recall	0.35	0.49	0.74	0.89	0.94
	Precision	0.34	0.49	0.51	0.96	0.96
	F-measure	0.35	0.49	0.61	0.91	0.95
Real	Recall	0.46	0.53	0.51	0.83	0.88
	Precision	0.44	0.87	0.51	0.97	0.97
	F-measure	0.45	0.66	0.51	0.90	0.93

Table 2: Image-level based performance of defect detection: comparison of 5 methods.

	Defect type	Detection Rate(%)
PG-LSR	Synthesized	48
	Real	65
PHOT	Synthesized	66
	Real	50
PN-RPCA	Synthesized	66
	Real	80
MPPC	synthesized	98
	Real	100
MPPC+Modification	synthesis	98
	Real	100

For image based performance evaluation (Ngan et al., 2011), we utilized the detection rate and the false alarm rate as follows:

$$\textit{Detection Rate} = \frac{N_T}{N_{TD}} \tag{14}$$

$$\textit{False Alarm Rate} = \frac{N_F}{N_{TF}} \tag{15}$$

where N_T, N_F, N_{TD} and N_{TF} are the numbers of defective logotypes or images correctly detected, defect-free detected as defective, the total number of defective samples, and defect-free logotypes, respectively.

4.3 Experimental Result

Many researchers carrying out defect detection for surface inspection have commonly examined steel (Selvi and Jenefa, 2014; Zhou et al., 2017), textile (Li et al., 2017; Arnia and Munadi, 2015), and wood (Zhang et al., 2015). For printing inspections, examinations have generally been performed with paper materials (Fucheng et al., 2009) and pharmaceutical capsules (Mehle et al., 2016). However, to our knowledge, no studies have investigated defect detection for logotypes on 3D micro-textured surfaces, as we have examined in the present study. To verify the effectiveness of the proposed method, we compared it and the original MPPC method with 3 methods: prior knowledge guided least squares regression (PG-LSR) for fabric defect inspection (Cao et al., 2017), phase only transform (PHOT) for surface defect detection (Aiger and Talbot, 2012), and modified robust principal component analysis with noise term and defect prior (PN-RPCA) for fabric inspection (Cao et al., 2016). All 3 methods are unsupervised. Also, they are very effective for detecting defects in textured material. The texture of the material they process is somewhat similar to the material mentioned in this paper. Furthermore, all of three methods disclose their source code and indicate the setting of the parameters.

Here, we used 60 synthesized defect images taken under the 3 different illumination conditions mentioned above and 20 real defect images of each character for comparison. Their implementation were conducted by use of the source code disclosed, and the selection of parameters were the recommended ones by the authors, respectively. Fig. 6 and Fig. 7 show representative results for the synthesized and real defects, respectively. Although fluctuations in illumination were large, we found that the proposed method could detect defects of very similar size and shape. This demonstrates that the OC in the MPPC models were highly robust. Furthermore, approximately half of the defects detected by all 4 methods were roughly consistent with the ground truth. For defects with high contrast, all the methods showed good detection performance. However, for low-contrast defects, PG-LSR, PHOT, and PN-RPCA showed lower performance than the proposed method. This is due to how the target materials used in the experiments were sufficiently different from those that they were initially designed for, which have somewhat consistent textures. The textures of our materials were generally random with irregular patterns. Table 1 shows the pixel-level based performance evaluation, while Table 2 shows the image-based performance evaluation for each method. These tables show that PG-LSR could successfully detect about half of all defects and that PHOT and PN-RPCA could successfully detect about 70% of all defects. The performance of the proposed method was very high. Furthermore, the MPPC with modification showed obvious improvement compared with the original MPPC.

5 CONCLUSIONS

We have proposed a novel model of statistical structure, the MPPC model, using orientation codes in defect-free logotypes printed on a 3D micro-textured surface. Based on the MPPC models of defect-free images, we proposed a new defect localization algorithm, which was effective for detecting defects in real images. From this, we also proposed a modified version of the MPPC. Our experimental results showed that the modified MPPC was an obvious improvement over the original MPPC.

In future works, we hope to design schemas to identify and classify different defect types, which may contribute to improving the effectiveness of QC in manufacturing production lines.

REFERENCES

Aiger, D. and Talbot, H. (2012). The phase only transform for unsupervised surface defect detection. In *Emerging Topics In Computer Vision And Its Applications*, pages 215–232. World Scientific.

Arnia, F. and Munadi, K. (2015). Real time textile defect detection using glcm in dct-based compressed images. In *Modeling, Simulation, and Applied Optimization (ICMSAO), 2015 6th International Conference on*, pages 1–6. IEEE.

Cao, J., Wang, N., Zhang, J., Wen, Z., Li, B., and Liu, X. (2016). Detection of varied defects in diverse fabric images via modified rpca with noise term and defect prior. *International Journal of Clothing Science and Technology*, 28(4):516–529.

Cao, J., Zhang, J., Wen, Z., Wang, N., and Liu, X. (2017). Fabric defect inspection using prior knowledge guided least squares regression. *Multimedia Tools and Applications*, 76(3):4141–4157.

Fucheng, Y., Lifan, Z., and Yongbin, Z. (2009). The research of printing's image defect inspection based on machine vision. In *Mechatronics and Automation, 2009. ICMA 2009. International Conference on*. IEEE.

Jing, J., Chen, S., and Li, P. (2015). Automatic defect detection of patterned fabric via combining the optimal gabor filter and golden image subtraction. *Journal of Fiber Bioengineering and Informatics*, 8(2):229–239.

Karimi, M. H. and Asemani, D. (2013). A novel histogram thresholding method for surface defect detection. In *2013 8th Iranian Conference on Machine Vision and Image Processing (MVIP)*, pages 95–99. IEEE.

Kasi, M. K., Rao, J. B., and Sahu, V. K. (2014). Identification of leather defects using an autoadaptive edge detection image processing algorithm. In *2014 International Conference on High Performance Computing and Applications (ICHPCA)*, pages 1–4. IEEE.

Li, M., Cui, S., Xie, Z., et al. (2015). Application of gaussian mixture model on defect detection of print fabric. *Journal of Textile Research*, 36(8):94–98.

Li, P., Liang, J., Shen, X., Zhao, M., and Sui, L. (2017). Textile fabric defect detection based on low-rank representation. *Multimedia Tools and Applications*, pages 1–26.

Liang, D., Hashimoto, M., Iwata, K., Zhao, X., et al. (2015). Co-occurrence probability-based pixel pairs background model for robust object detection in dynamic scenes. *Pattern Recognition*, 48(4):1374–1390.

Mardia, K. V. (1970). Measures of multivariate skewness and kurtosis with applications. *Biometrika*, 57(3):519–530.

McHugh, M. L. (2013). The chi-square test of independence. *Biochemia medica: Biochemia medica*, 23(2):143–149.

Mehle, A., Bukovec, M., Likar, B., and Tomaževič, D. (2016). Print registration for automated visual inspection of transparent pharmaceutical capsules. *Machine Vision and Applications*, 27(7):1087–1102.

Ngan, H. Y., Pang, G. K., and Yung, N. H. (2011). Automated fabric defect detection- a review. *Image and Vision Computing*, 29(7):442–458.

Selvi, M. and Jenefa, D. (2014). Automated defect detection of steel surface using neural network classifier with co-occurrence features. *International Journal*, 4(3).

Ullah, F. and Kaneko, S. (2004). Using orientation codes for rotation-invariant template matching. *Pattern recognition*, 37(2):201–209.

Xiang, S., Yan, Y., Asano, H., and Kaneko, S. (2018). Robust printing defect detection on 3d textured surfaces by multiple paired pixel consistency of orientation codes. In *2018 12th France-Japan and 10th Europe-Asia Congress on Mechatronics*, pages 373–378. IEEE.

Xie, X. (2008). A review of recent advances in surface defect detection using texture analysis techniques. *ELCVIA Electronic Letters on Computer Vision and Image Analysis*, 7(3).

Zhang, Y., Xu, C., Li, C., Yu, H., and Cao, J. (2015). Wood defect detection method with pca feature fusion and compressed sensing. *Journal of forestry research*, 26(3):745–751.

Zhou, S., Chen, Y., Zhang, D., Xie, J., and Zhou, Y. (2017). Classification of surface defects on steel sheet using convolutional neural networks. *Mater. Technol*, 51(1):123–131.